

## Efficient synthesis of xanthene derivatives in aqueous media in the presence of Cu-anchored furfural imine-functionalized halloysite

Samahe Sadjadi\*

Gas Conversion Department, Faculty of Petrochemicals, Iran Polymer and Petrochemical Institute, PO Box 14975-112, Tehran, Iran.

Received 22 December 2016; received in revised form 6 April 2017; accepted 15 June 2017

### ABSTRACT

A novel hybrid catalyst based on grafting Cu on furfural imine-functionalized halloysite was designed, characterized and used for promoting synthesis of xanthene derivatives via three- component reaction of benzaldehyde derivatives, dimedone, and  $\beta$ -naphthol in aqueous media and under mild reaction condition. The results established high catalytic activity of the hybrid system, which was superior to some conventional catalysts. Moreover, the catalyst was reusable and could be easily recovered and reused for several reaction runs with slight loss of catalytic activity. Broad substrate scope, simple work up procedure and performing the process in aqueous media are other merits of this protocol.

**Keywords:** Halloysite Clay, Catalyst, Xanthenes, Heterogeneous, Cu-based catalysts.

### 1. Introduction

Xanthenes and heterocycles containing xanthenes fragment can be found in natural products and exhibit biological activities [1] such as antibacterial and antiviral activities [2] and anti-inflammatory [3]. Besides biological properties, the attractive spectroscopic properties of these heterocycles resulted in various applications in the field of photo dynamic therapy [4], visualization of biomolecules [5] and laser technology [6]. All these interesting features and uses of xanthenes led to numerous attempts for developing facile and efficient methods for synthesis of various xanthenes derivatives [4, 7-10].

Halloysite (Hal) nanotubes ( $\text{Al}_2(\text{OH})_4\text{Si}_2\text{O}_5 \cdot 2\text{H}_2\text{O}$ ) are naturally occurring hydrated polymorph of kaolinite with similar chemical and structural features to those of kaoline [11-14]. However, in Hal a  $\text{H}_2\text{O}$  monolayer separates the unite layers. Hal nanotubes have attracted growing attention and applications in various research fields such as catalysis [15], membrane for gas separation [16], photodegradation [17], water treatment [18], and drug delivery [19-21] due to their unique

properties such as high specific surface area, specific meso/macrosopic superstructure of Hal [11] and cation exchange capacities. Recently, functionalization of Hal with various functional groups has been reported [22].

In the last decade, we tried to develop new heterogeneous catalysts for synthesis of heterocycles such as coumarin [23], pyrimidines [24] and fused heterocycles such as benzochromeno-pyrazole and pyrazolopyranopyrimidines [25].

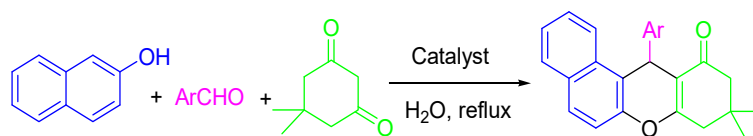
In continuation of our attempts, herein we wish to report for the first time a novel hybrid catalytic system based on grafting Cu on furfural imine-functionalized Hal and study the catalytic performance of the catalyst for the synthesis of xanthene derivatives via three-component reaction of benzaldehydes, dimedone, and  $\beta$ -naphthol in aqueous media and mild reaction time (Scheme 1).

### 2. Experimental

#### 2.1. Amine functionalization of Hal: A-Hal

Hal was amine functionlized through a previously reported protocol [11]. Typically, 4 mL (3-aminopropyl)triethoxysilane, APTES, was added to the suspension of 1.2 g Hal in dry toluene.

\*Corresponding author email: samahesadjadi@yahoo.com  
Tel: +98 21 4866 2478; Fax: +98 21 4478 7021



**Scheme 1.** Synthesis of xanthenes derivaives.

The mixture was homogenized using ultrasonic irradiation for 0.5 h and then refluxed for 24h. The obtained precipitate was separated and washed repeatedly with dry toluene. The amine functionalized Hal, A-Hal, was furnished after drying the filtrate at 110 °C for 12h.

### 2.2. Imine functionalization of Hal: I-Hal

Furfural was dissolved in methanol (5 cc) and added drop wisely into the stirring suspension of A-Hal in 30 cc methanol. The mixture was then refluxed for 18h. Upon condensation reaction, the color of the mixture changed into deep yellow. After completion of the reaction, the resulting precipitate was filtered, washed several times with hot methanol and dried at 90 °C for 12h.

### 2.3. Synthesis of Cu(II) anchored Hal: Cu-I-Hal

Copper (II) acetate (0.4 g) was added to the suspension of I-Hal (2g) in ethanol (30 cc). Subsequently, the mixture was refluxed for 18h. The color of the reaction mixture turned into green. Upon completion of the reaction, the product was filtered and washed with ethanol repeatedly. The final catalyst, Cu- I-Hal, was achieved by drying the precipitated at 100 °C for 12h (Scheme 2).

### 2.4. Synthesis of xanthenes: General procedure

To an aqueous mixture of an dimedone (1 mmol), benzaldehydes (1 mmol) and  $\beta$ -naphthol (1 mmol), catalytic amount of the catalyst (0.03 g) was added. Subsequently, the mixtur was refluxed for an

appropriate time. Upon completion of the process, monitored by TLC, the mixture was cooled to ambient temperature and the obtained percipitate was filtered off, washed repeatedly with H<sub>2</sub>O and purified by recrystallization from absolute ethanol. All products were known compounds and identified by comparison of their physical and spectroscopic data with those of authentic samples which found being identical.

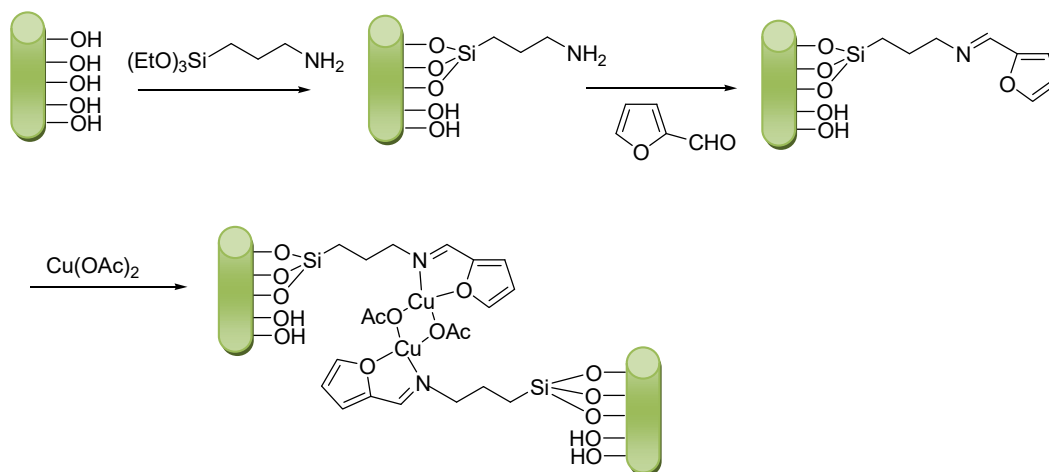
### 2.5. Catalyst characterization

The Cu- I-Hal catalyst was characterized by applying XRD, SEM/EDX, Elemental mapping analysis and FTIR techniques. SEM/EDX as well as elemental mapping analyses were performed by a Tescan instrument, using Au-coated samples and acceleration voltage of 20 kV. FTIR spectra were recorded by using PERKIN-ELMER- Spectrum 65 instrument. Room temperature powder X-ray diffraction patterns were collected using a Siemens, D5000. CuK $\alpha$  radiation was used from a sealed tube. Data were collected in the 2 $\theta$  range of 10–75° with a step size of 0.02° and an exposure time of 2s per step.

## 3. Results and Discussion

### 3.1. Characterization of catalysts

The FTIR spectrum of the catalyst is depicted in Fig. 1. The characteristic peaks at 3695.1 and 3625.2 cm<sup>-1</sup> are assigned to internal and external hydroxyl groups of Hal, while the observed peaks at 2928 and 1039 cm<sup>-1</sup> are attributed to -CH<sub>2</sub> stretching and Si-O stretching [26].



**Scheme 2.** Catalyst synthetic procedure.

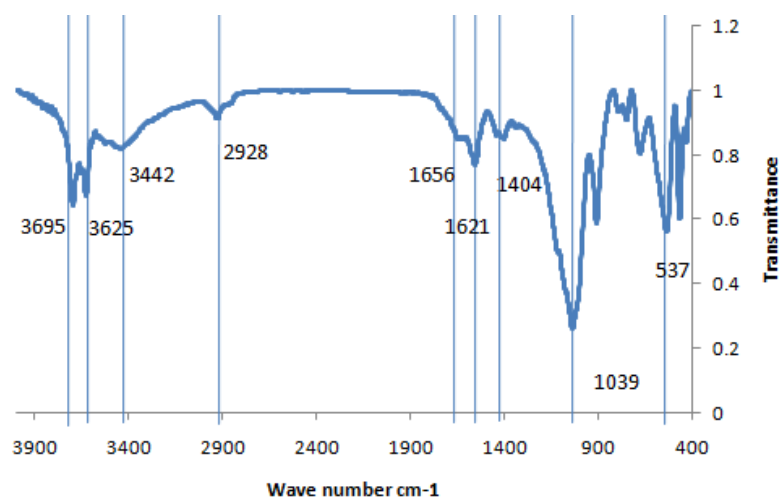


**Fig. 1.** FTIR spectrum of Cu-I-Hal.

The Al-O-Si vibration and the interlayer water can be detected at 537 and 1656  $\text{cm}^{-1}$ . The peak at 3442  $\text{cm}^{-1}$  which is due to stretching vibration of N-H can prove the attachment of APTES. Coordination of Cu can be confirmed by observing two peaks at 573 and 1404  $\text{cm}^{-1}$  which can be attributed to the asymmetric and symmetric vibrations, respectively, of the bridging acetate ions. Moreover, the peak at 1621  $\text{cm}^{-1}$  can be assigned to imine functional group. The observed shift of imine band to lower wavelength can be the result of coordination to Cu [27].

The SEM/EDX analyses of the synthesized catalyst are illustrated in Fig. 2. As obvious the SEM images of Cu-I-Hal is distinguished from the bare Hal (Fig. 2). The nanotubes in bare Hal form aggregate. In Cu-I-Hal, however, the tubular morphology is changed to intertwine one. The presence of Al, Si and O elements in EDX analysis can be assigned to Hal structure, while the C and N can prove the conjugation of APTES. Obviously, the Cu is present in the structure of the catalyst.

Elemental mapping analysis was also exploited for investigating the structure of the catalyst. The results establish almost uniform distribution of copper species on the catalyst. (Fig. 3).

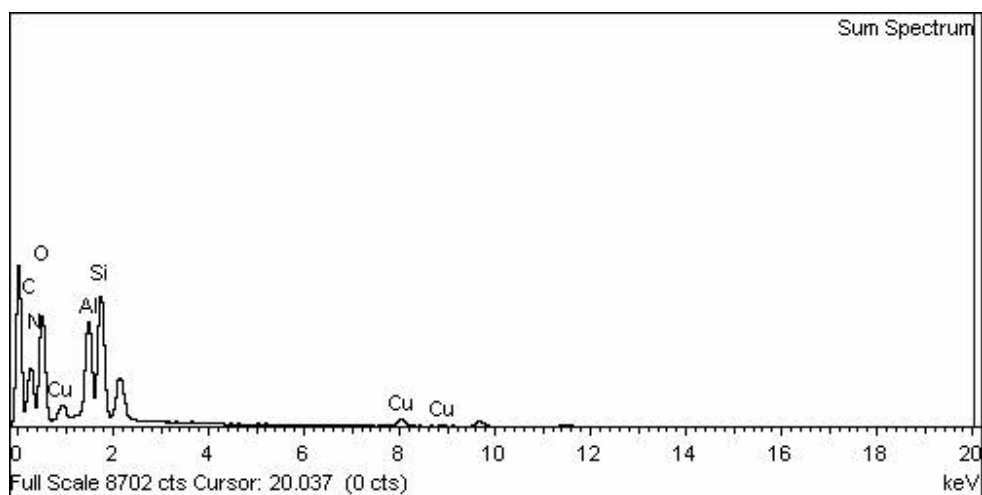
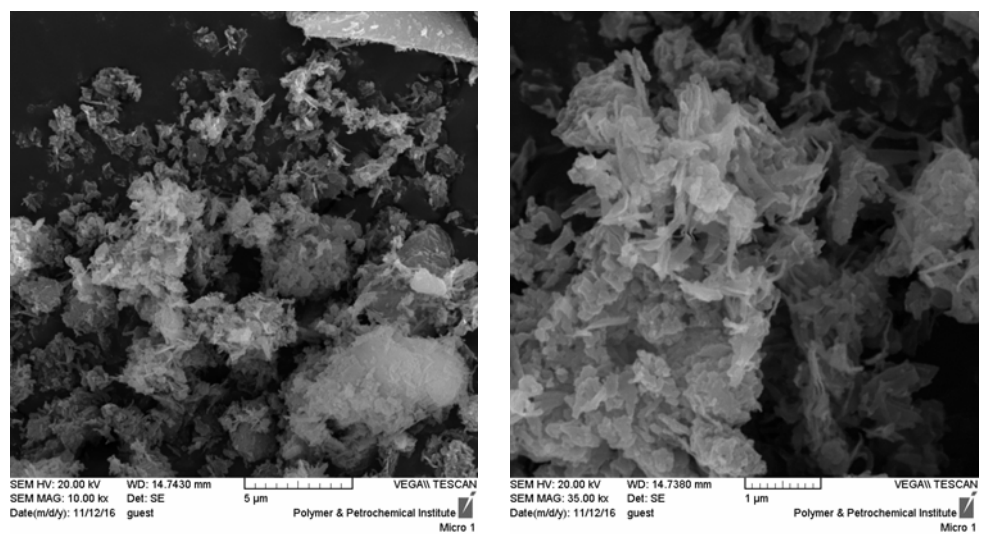
According to the previous reports, all of the peaks in the XRD pattern can be assigned to the characteristic peaks of Hal [11,14]. No distinguished peak was observed for copper. According to the literature, this can be due to [28] the low amount of copper and its high dispersion. A proof for incorporation of copper is the observed shift of the Hal peaks to higher value of  $2\theta$ . This can establish the attachment of the copper sites on the surface of functionalized Hal [29-30]. (Fig. 4)

### 3.2. Catalytic activity

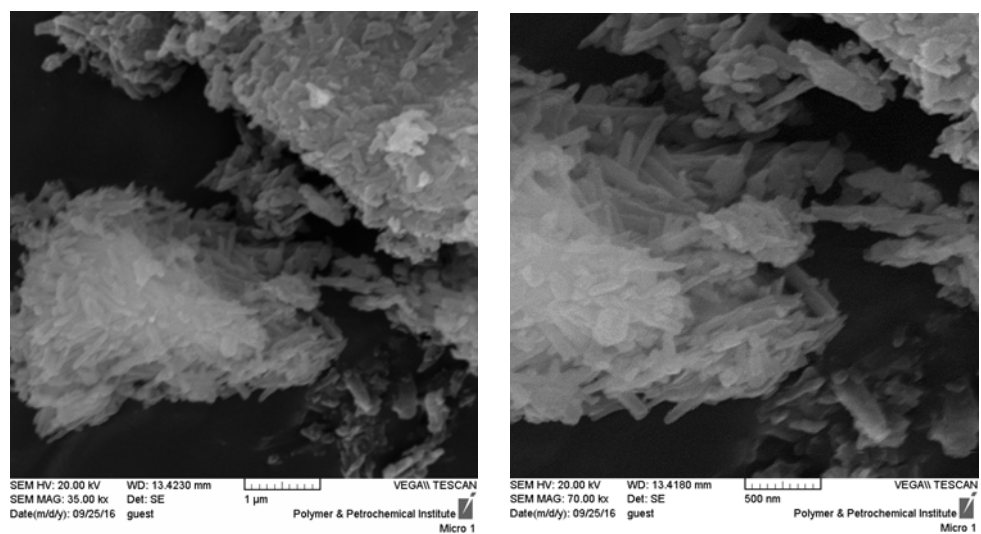
In our previous attempt to develop a novel catalyst for the of xanthene derivatives, we introduced the heteropolyacids immobilized on cyclodextrin nanosponges [31]. Although the results were promising and the reaction could proceed in aqueous media, the leaching of heteropolyacid was remained challenging. Recently, we disclosed the potential of Hal for developing heterogeneous catalysts [26]. In following of our attempt for introducing efficient and heterogeneous catalysts for ecofriendly processes for the synthesis of heterocycles, we designed and synthesized a novel catalyst based on incorporation of Cu catalytic species on amine functionalized Hal.

Initially, the reaction of benzaldehyde, dimedone and  $\beta$ -naphthol was selected as a model reaction to investigate the catalytic potential of the catalyst and optimization of the reaction variables. To this purpose, the model reaction was performed using various amounts of the catalyst (0.02-0.07g), in various solvents including water, EtOH,  $\text{CH}_3\text{CN}$  and toluene under reflux and stirrer condition. The results established that performing the reaction in water under reflux condition in the presence of 0.03 g catalyst led to the best yield (Table 1).

Knowing the optimum reaction condition, the reaction was carried out using various aldehydes with different electron densities. The results demonstrated that both electron rich and electron deficient aldehydes could tolerate the reaction to furnish the corresponding xanthenes in high yields (Table 2). However, the aldehydes with electron withdrawing groups could afford the products in slightly higher yields.



A



B

Fig. 2. A: SEM/EDX image of Cu- I-Hal and B: SEM image of HNTs [26].

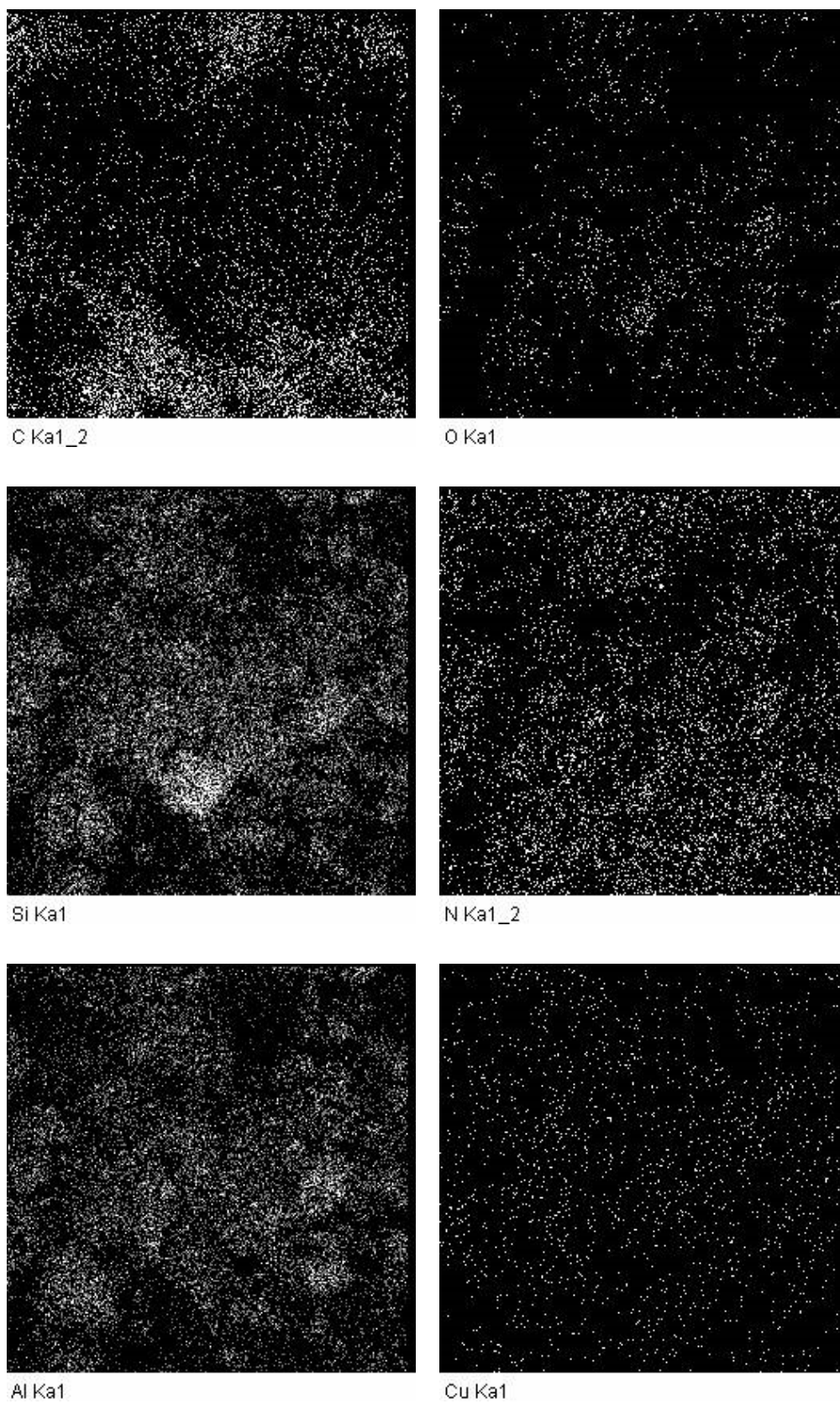
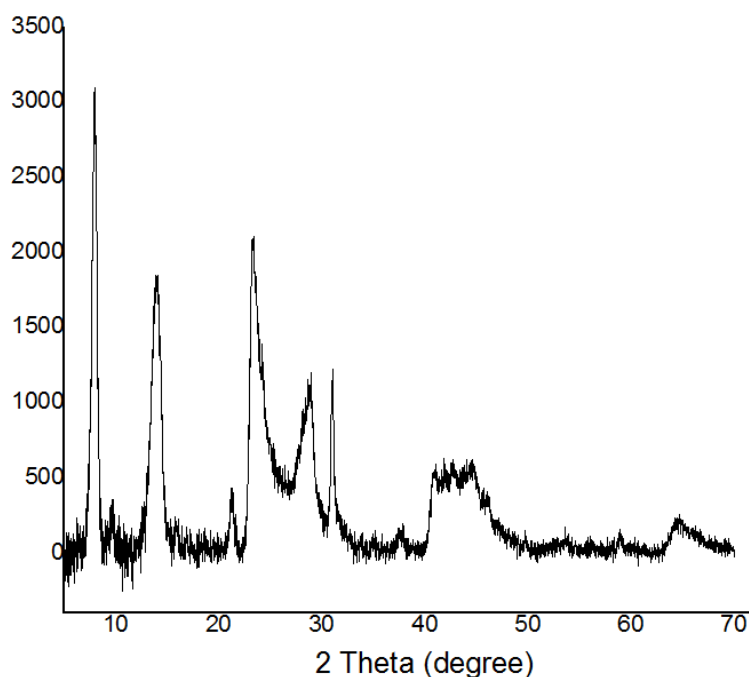


Fig. 3. Elemental mapping analysis of Cu- I-Hal.



**Fig. 4.** XRD pattern of Cu- I-Hal.

Regarding the reaction mechanism and the role of the catalyst in promoting the reaction, it is proposed that Hal nanotubes which possess the Bronsted acidity and copper species can activate the carbonyl group and accelerate the Knoevenagel condensation to afford an intermediate. The latter subsequently tolerated the reaction with  $\beta$ -naphthol which can be catalyzed with acidic catalyst, intermolecular cyclization and dehydration (Scheme 3). To investigate the catalytic activity of the novel hybrid catalyst for promoting the

three -component reaction and synthesis of xanthenes, the model compound was synthesized in the presence of various conventional catalysts including DABCO, sulfamic acid, PEG-400, Ceric ammonium nitrate,  $I_2$ ,  $NaHSO_4-SiO_2$ ,  $Sr(OTf)_2$ , *p*-toluenesulfonic acid, Keggin, Preyssler types of heteropolyacids (HPA), bare Hal and our previously reported catalysts, i.e. cyclodextrin nanosponges (CD), HPA embedded CD, HPA-CDNS, and HPA embedded in amine functionalized CD, HPA-CDNS/ $NH_2$  (Table 3).

**Table 1.** Effect of various solvents and catalyst amount on the synthesis of the model reaction in the presence of novel catalyst.

Entry	Solvent	Time (min)	Catalyst amount (g)	Yield (%) <sup>a</sup>
1	H <sub>2</sub> O	50	0.05	92
2	CH <sub>3</sub> CN	60	0.05	80
3	CH <sub>2</sub> Cl <sub>2</sub>	80	0.05	75
4	DMF	120	0.05	70
5	EtOH	60	0.05	85
6	Toluene	120	0.05	60
7	H <sub>2</sub> O	75	0.02	80
8	H <sub>2</sub> O	60	0.04	88
9	H <sub>2</sub> O	50	0.07	92

<sup>a</sup>Yields refer to isolated products.

**Table 2.** Synthesis of xanthene derivatives using a catalytic amount of Cu- I-Hal.

Entry	Ar	Yield (%) <sup>a</sup>	Time (min)	m.p (°C)	
				Found	Reported <sup>b</sup>
1	C <sub>6</sub> H <sub>5</sub>	92	50	153-155	154-155
2	4-Br-C <sub>6</sub> H <sub>4</sub>	96	45	184-186	185-187
3	4-Cl-C <sub>6</sub> H <sub>4</sub>	97	45	185-187	186-188
4	3-NO <sub>2</sub> -C <sub>6</sub> H <sub>4</sub>	95	45	182-185	183-184
5	4-MeO-C <sub>6</sub> H <sub>4</sub>	92	55	189-201	200-202
6	4-NO <sub>2</sub> -C <sub>6</sub> H <sub>4</sub>	95	45	170-172	172-174
7	3-MeO-C <sub>6</sub> H <sub>4</sub>	89	60	202-203	204-205
8	2-Me-C <sub>6</sub> H <sub>4</sub>	90	55	159-160	159-162
7	2,4-Cl <sub>2</sub> -C <sub>6</sub> H <sub>3</sub>	94	40	213-214	214-215

<sup>a</sup> Isolated yields.<sup>b</sup> All from ref. [8].

As obvious, Cu-I-Hal exhibited superior catalytic activity compared to bare Hal, this can suggest the synergistic effects between the Hal and the second catalytic species, copper [26]. Not only the catalytic activity of the Cu-I-Hal was higher than homogeneous catalysts such as HPA, DABCO, *p*-toluenesulfonic acid and sulfamic acid, but also its heterogeneous nature renders Cu-I-Hal reusable. Compared to all tabulated catalysts, Cu-I-Hal could lead to the desired product in shorter reaction time.

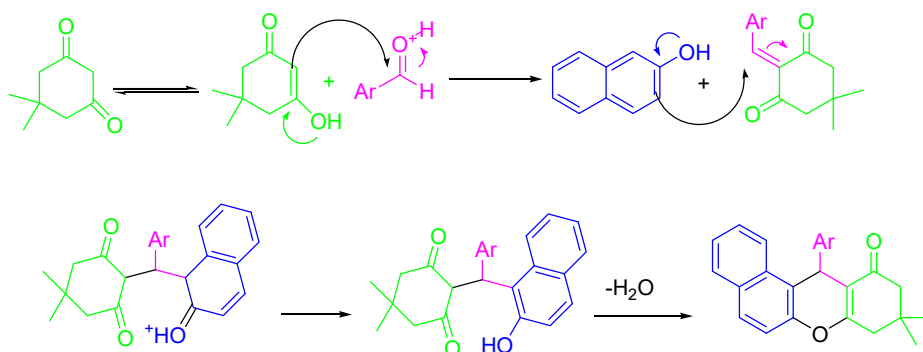
### 3.3. Catalyst reusability

The reusability of the hybrid catalytic system was examined by performing the model reaction in the presence of the reused catalyst. As obvious, upon recovering and reusing the catalyst, only slight loss of the catalytic activity was observed. Using hot filtration method, it was established that the leaching amount of

the copper species was negligible. This result established the heterogeneous nature of the catalysis and ruled out the homogeneous catalysis emerged from the leached copper species in the solvent. The yields for four reaction runs were 92, 90, 88 and 87%, respectively.

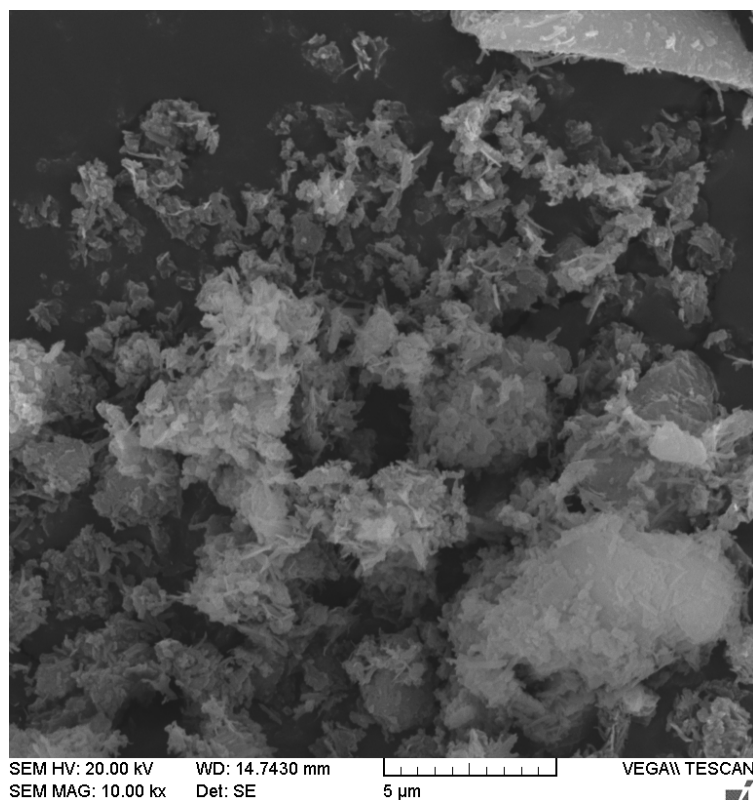
To study whether reusing of the catalyst alter its properties, the reused catalyst was characterized by using SEM, FTIR and XRD analyses. The SEM image of the re-used catalyst, Fig. 5, established that the catalyst preserved its morphology upon reusing.

The XRD patterns of the fresh and reused catalysts were also compared (Fig. 6). The results implied the identical XRD patterns, indicating that the phases in these two catalysts are similar and reusing of the catalyst did not induce any phase change in the catalyst.

**Scheme 2.** The plausible mechanism of the xanthene synthesis.

**Table 3.** The catalytic activities of various catalysts for the synthesis of model xanthenes under reflux condition.

Entry	Catalyst	Solvent	Temp.	Time	Yield (%)	Ref.
1	$H_{14}NaP_5W_{30}O_{110}$	Water	Reflux	2 h	79	This work
2	$H_4[Mo_{12}PO_{40}]$	Water	Reflux	2 h	81	This work
3	DABCO	Water	Reflux	4 h	60	This work
4	CDNS	Water	Reflux	3.5 h	70	[31]
5	HPA-CDNS	Water	Reflux	2.5 h	88	[31]
6	HPA-CDNS/ $NH_2$	Water	Reflux	60min	91	[31]
7	Sulfamic acid	Water	Reflux	3h	79	This work
8	Hal	Water	Reflux	80 min	80	This work
9	$NaHSO_4-SiO_2$	$ClCH_2CH_2Cl$	Reflux	4h	87	[32]
10	$Sr(OTf)_2$	$ClCH_2CH_2Cl$	80 °C	5h	85	[33]
11	<i>p</i> -toluenesulfonic acid	-	$[bmim]BF_4$ , 80 °C	3h	90	[34]
12	$I_2$	ACOH	Reflux, 80 °C	2.5h	87	[35]
13	PEG-400	-	120 °C	6.5h	87	[36]
14	Ceric ammonium nitrate	DCM-ethanol	Ultrasound	120m	85	[37]
15	Cu-I-Hal	Water	Reflux	50min	92	This work

**Fig. 5.** The SEM image of the reused catalyst.



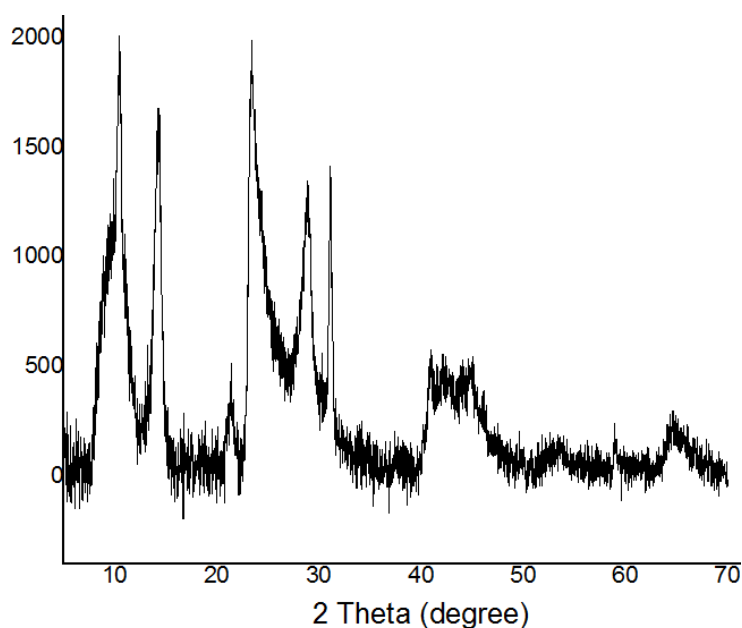


Fig. 6. XRD pattern of the reused catalyst.

The FTIR analysis of the reused catalyst (Fig. 7) also prove that re-using of the catalyst did not alter its structure and the characteristic bands for the fresh catalyst, discussed in section 2.1, can be detected for the reused catalyst too. The identical physical properties of fresh and reused catalysts can justify their similar catalytic activities. In the other word, the morphology of the catalyst, the phases and other structural properties of a catalyst can play roles in the catalytic activity. As reusing the catalyst did not cause any change in phase, chemical composition and catalyst active phases, it is expected that fresh and reused catalysts exhibited similar catalytic activities.

### Conclusion

In summary, a novel hybrid catalytic system based on grafting Cu on furfural imine-functionalized halloysite was introduced and used for catalyzing synthesis of xanthene derivatives via three-component reaction in aqueous media and mild reaction condition. Broad substrate scope, simple work up procedure, reusability of the catalyst, high yields and performing the process in aqueous media are the merits of this protocol for synthesis of xanthenes.

### Acknowledgment

The authors appreciate partial financial supports from Iran Polymer and Petrochemical Institute.

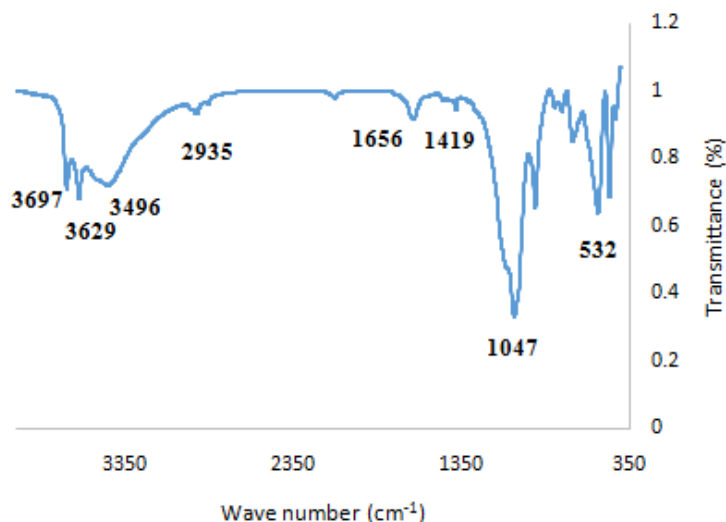


Fig. 7. FTIR spectrum of the reused catalyst.

## References

- [1] A. Gharib, L. Vojdani Fard, N.N. Pesyan, M. Roshani, *Chem. J.* 1 (2015) 58-67.
- [2] R.M. Ion, D. Frackowiak, K. Wiktorowicz, *Acta Biochim. Pol.* 45 (1998) 833-845.
- [3] J.M. Jamison, K. Krabill, A. Hatwalkar, *Cell. Biol. Int. Rep.* 14 (1990) 1075-1084.
- [4] P. Bansal, G.R. Chaudhary, N. Kaur, S.K. Mehta, *RSC Adv.* 5 (2015) 8205-8209.
- [5] O. Evangelinou, A.G. Hatzidimitriou, E. Velalib, A.A. Pantazaki, N. Voulgarakis, P. Aslanidis, *Polyhedron* 72 (2014) 122-129.
- [6] O. Sirkecioglu, N. Talinli, A. Akar, *J. Chem. Res.* (1995) 502-506.
- [7] G.R. Chaudhary, P. Bansal, N. Kaur, S.K. Mehta, *RSC Adv.* 4 (2014) 49462-49470.
- [8] M. M. Heravi, H. Alinejhad, K. Bakhtiari, M. Saeedi, H. A. Oskooie, F. F. Bamoharram, *Bull. Chem. Soc. Ethiop.* 25 (2011) 399-406.
- [9] K. Rad-Moghadam, S.K. Azimi, *J. Mol. Catal. A: Chem.* 363-364 (2012) 465-469.
- [10] N.G. Khaligh, *Ultrason. Sonochem.* 19 (2012) 736-739.
- [11] P. Yuan, P.D. Southon, Z. Liu, M.E.R. Green, J.M. Hook, S.J. Antill, C.J. Kepert, *J. Phys. Chem. C* 112 (2008) 15742-15751.
- [12] Y. Zhang, J. Ouyang, H. Yang, *Appl. Clay Sci.* 95 (2014) 252-259.
- [13] Y. Zhang, A. Tang, H. Yang, *J. Ouyang, Appl Clay Sci.* 119 (2016) 8-17.
- [14] H. Zhu, M.L. Du, M.L. Zou, C.S. Xu, Y.Q. Fu, *Dalton Trans.* 41 (2012) 10465-10471.
- [15] P. Djomgoue, D. Njopwouo, *J. Surf. Eng. Mater. Adv. Technol.* 3 (2013) 275-282.
- [16] R.S. Murali, M. Padaki, T. Matsuura, M.S. Abdullah, A.F. Ismail, *Sep. Purif. Technol.* 132 (2014) 187-194.
- [17] B. Szczepanik, P. Słomkiewicz, *Appl Clay Sci.* 124-125 (2016) 31-38.
- [18] D. Grabka, M. Raczyńska-Żak, K. Czech, P.M. Słomkiewicz, M.A. Józwiak, *Appl Clay Sci.* 114 (2015) 321-329.
- [19] Y. Zhang, H. Yang, *Phys. Chem. Miner.* 39 (2012) 789-795.
- [20] M. Guo, A. Wang, F. Muhammad, W. Qi, H. Ren, Y. Guo, G. Zhu, *Chin. J. Chem.* 30 (2012) 2115-2120.
- [21] L. Sun, D.K. Mills, *Conf. Proc. IEEE Eng. Med. Biol. Soc.* 2014 (2014) 2920-2923.
- [22] P. Pasbakhsh, G.J. Churchman, First Ed., Apple Academic Press, Oakville, 2015.
- [23] M.M. Heravi, S. Sadjadi, S. Sadjadi, H.A. Oskooie, F.F. Bamoharram, *Ultrason. Sonochem.* 16 (2009) 708-710.
- [24] M.M. Heravi, S. Sadjadi, H.A. Oskooie, Rahim Hekmat Shoar, F.F. Bamoharram, *Tetrahedron Lett.* 50 (2009) 662-666.
- [25] M.M. Heravi, M. Saeedi, Y.S. Beheshtiha, H.A. Oskooie, *Mol. Divers.* 15 (2011) 239-243.
- [26] S. Sadjadi, M.M. Heravi, M. Daraie, *Res. Chem. Intermed.* 43 (2017) 2201-2214.
- [27] J. Mondal, A. Modak, A. Dutta, S. Basu, S. Nath Jha, D. Bhattacharyya, A. Bhaumik, *Chem. Commun.* 48 (2012) 8000-8002.
- [28] S. Mallik, S.S. Dash, K.M. Parida, B.K. Mohapatra, *J. Colloid Interface Sci.* 300 (2006) 237-243.
- [29] P. Bhanja, R. Gomes, L. Satyanarayana, A. Bhaumik, *J. Mol. Catal. A: Chem.* 415 (2016) 104-112.
- [30] J. Mondal, P. Borah, A. Modak, Y. Zhao, A. Bhaumik, *Org. Process Res. Dev.* 18 (2014) 257-265.
- [31] S. Sadjadi, M.M. Heravi, M. Daraie, *Res. Chem. Intermed.* 43 (2017) 843-857.
- [32] B. Das, K. Laxminarayana, M. Krishnaiah, Y. Srinivas, *Synlett* (2007) 3107-3112.
- [33] J. Li, W. Tang, L. Lu, W. Su, *Tetrahedron Lett.* 49 (2008) 7117-7120.
- [34] J. M. Khurana, D. Magoo, *Tetrahedron Lett.* 50 (2009) 4777-4780.
- [35] X. J. Sun, J. F. Zhou, P. S. Zhao, *Synth. Commun.* 42 (2012) 1542-1549.
- [36] N.V. Shitole, S.B. Sapkal, B.B. Shingate, M.S. Shingare, *Bull. Korean Chem. Soc.* 32 (2011) 35-36.
- [37] S. Sudha, M. A. Pasha, *Ultrason. Sonochem.* 19 (2012) 994-998.